

## El Niño Iterations\*

Klaus Fraedrich\*\*

Bureau of Meteorology Research Centre, Melbourne, Victoria 3001, Australia

(Manuscript received 26.06.1986, in revised form 07.10.1986)

### Zusammenfassung: El Niño Iterationen

Eine empirische (quadratische) Iteration dient der Beschreibung von jährlich beobachteten El Niño Intensitäten, wobei die thermische Trägheit des Ozeans als externer Parameter variiert wird. Dieses Konzept der Klima-Iteration (und nicht die diskrete Version einer kontinuierlichen Entwicklung) wird am Beispiel des El Niño dargestellt: Die Iteration zeigt einen Attraktionsbereich sowie darin eingebettet (invariante) Intervalle, aus denen das System nicht entkommen kann. Die zeitliche Entwicklung zeigt die bekannten Merkmale der Periodenverdopplung bei Änderung des externen Parameters. Stochastische Störungen verwischen die Struktur der Iteration; mit zunehmender Intensität erweitern sie den Parameterbereich, der durch irreguläre Entwicklung gekennzeichnet ist. Allerdings bleiben der Attraktionsbereich und die invarianten Intervalle beinahe unverändert.

### Abstract:

An empirical (quadratic) temperature iteration is deduced from observed annual El Niño/Southern Oscillation intensities with the thermal inertia or ocean surface layer depth representing the external or bifurcation parameter. This leads to the concept of an iterative (and not the discrete version of a continuous) climate system, the dynamics of which is analysed: (i) The structural analysis of the system emphasizes a basin of attraction and embedded intervals, from which the time evolution of the system cannot escape. (ii) Further details of the time evolution reveal the known features of period doubling. (iii) Stochastic forcing diffuses the iterations and enhances the parameter domain of irregularity with increasing noise level; but the main stability properties with the attractor basin and invariant interval remain almost unchanged.

### Résumé: Itérations sur El Niño

Une itération empirique (quadratique) décrit les intensités annuelles du phénomène El Niño en prenant comme paramètre externe de bifurcation l'inertie thermique des océans. Ceci conduit au concept d'un système itératif de climat (et non à une version discrète d'un continuum) dont on analyse la dynamique: (i) l'analyse structurelle du système montre l'existence d'une cuvette d'attraction et d'intervalles enchâssés où reste confinée l'évolution temporelle du système, (ii) des détails plus fins de l'évolution temporelle révèlent la caractéristique connue du doublement de période, (iii) une contrainte stochastique modifie la structure de l'itération et élargit le domaine paramétrique d'irrégularité avec accroissement du bruit mais les propriétés essentielles de stabilité associées à la cuvette de l'attracteur et à l'intervalle invariant restent presque inchangées.

\* dedicated to Prof. Dr. H. Flohn on the occasion of his 75th birthday

\*\* On leave from Institut für Meteorologie, Freie Universität Berlin.

## 1 Introduction

Simple climate systems represent the maximum truncation of the governing set of climate equations. These systems are generally reduced to a single state variable, but they keep a low-order nonlinearity. A typical example is the geometrically zero-dimensional climate model derived from the global energy balance; its state variable is the globally averaged temperature (e.g. FRAEDRICH, 1978, 1979). The time evolution of simple climate systems is commonly described by trajectories in the phase space, which are continuous in time and supposed to provide a smooth picture of reality; although catastrophes may occur if external parameters are changed, the time trajectories remain smooth and do not show chaotic behaviour. A more realistic time evolution of these simple systems is obtained by introducing random forces. They originate on a significantly smaller time scale and are essentially independent. This leads to a probabilistic chaos of the system due to forces, which are not explicitly resolved by the model (e.g. SUTERA, 1981; BENZI et al., 1981). Deterministic chaos may occur in nonlinear low order models describing the time evolution of at least three continuous state variables. One such example has recently been suggested by VALLIS (1986) for the El Nino/Southern Oscillation.

A qualitatively different approach towards climate modelling is the iterated climate system or climate iteration, which simulates a subset of the evolution of all climate variables in the phase space. This approach may be interpreted as a parameterization reducing a comprehensive climate system, which evolves continuously in a higher dimensional phase space, to a discrete climate iteration with one state variable only. For example, such a subset is a series of the lowest monthly mean temperatures of consecutive winter seasons; i.e. the complete set of climate variables is confined to a local temperature extremum of the natural annual cycle and the time evolution is reduced to a sequence of points. Another example, which is adopted in this paper, is the El Nino/Southern Oscillation phenomenon. If the annual intensities are calibrated with representative ocean temperatures and with the thermal inertia of an ocean surface layer, one can obtain a quadratic temperature iteration (Section 2). VALLIS' (1986) El Nino model and the El Nino iteration to be discussed have one qualitative feature in common: Successive maxima of one of the three variables in his model, which is closely related to the LORENZ model (1963, Figure 4), reveal an iteration with a single extremum.

In several ways a quadratic iteration is a general one, because locally every nonlinear map is quadratic. Therefore it is not surprising that this equation has a long tradition (i) to study "the problem of deducing the climate from the governing equations" (LORENZ, 1964), (ii) to show analogies with fluids passing from one regime of flow to another and (iii) to evaluate chaotic behaviour in nonlinear systems (MAY, 1976), which leads to fundamental laws (GROSSMANN and THOMAE, 1977; FEIGENBAUM, 1978) and to one scenario of turbulence (e.g. OTT, 1981; ECKMANN, 1981). Applied to the zero-dimensional climate iteration (Sections 3 and 4) the main goal is to evaluate its structural behaviour changing with the bifurcation parameter of the system.

## 2 An example: Iterations with El Niño intensities

A climate signal on time scales of months to years is the El Nino/Southern Oscillation phenomenon of the tropical ocean-atmosphere system. It is associated with sea surface temperature anomalies, which may exceed 4 degrees Celsius over large areas of the tropical Pacific, dislocations of rainfall in the tropics, circulation anomalies extending far into the middle and higher latitudes, etc. (e.g. RASMUSSEN and CARPENTER, 1982). Intensities of these events can be traced back into the 18th century; since 1861 it was possible to quantify El Nino events annually by four distinct classes of strong, moderate, weak and very weak intensities  $I$  (QUINN et al., 1978, updated by RASMUSSEN, 1984, Table 1). During the last 120 years from 1864 to 1883 one observes a (almost u-shaped) frequency distribution with 70 years of no events ( $0 \leq I \leq 1$ ), 6 very weak ( $1 < I \leq 2$ ), 8 weak ( $2 < I \leq 3$ ) and 35 years of moderate to

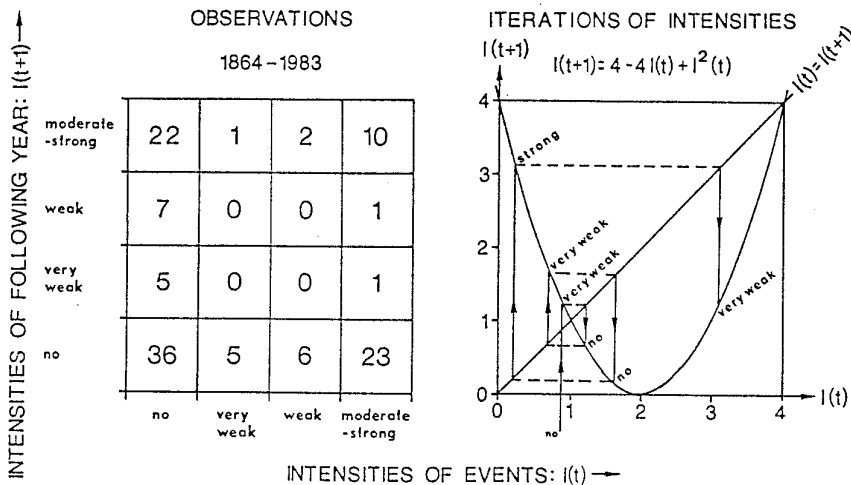
strong events combined ( $3 < I \leq 4$ ); here a continuous scale is associated with the intensities to make the transformation to a temperature scale tractable. The intensity record,  $I_t$ , can be displayed in a plane spanned by annual intensities,  $I_t$ , and those of the following year,  $I_{t+1}$ . This defines a phase portrait of the El Niño phenomenon, the dynamics of which is described by iterations in the  $(I_t, I_{t+1})$ -space. Such iterations can be visualized on appropriate cross-sections through a phase space, representing the continuous time evolution of the tropical climate system. Each iteration denotes an intersection of the continuous trajectory with this cross-section and the  $(t+1)$ st intersection is related to its predecessor, the  $t$ -th intersection. In this sense iterations describe discrete dynamics, which have nothing to do with the discretization process of the continuous time evolution equations; it is the discrete dynamics, which will be discussed in the following.

The 120 intensity values classify years, which are and are not effected by El Niño events. They are sampled in the  $(I_{t+1}, I_t)$ -plane (Fig. 1, left) and approximated by a continuous graph defined by a truncated power series:

$$I_{t+1} = M_0 + (M_1 + 1) I_t + M_2 I_t^2 + \dots \quad (2.1)$$

Only for a first qualitative discussion parameter values are chosen to be  $M_0 = 4$ ,  $M_1 + 1 = -4$  and  $M_2 = 1$ , (Figure 1, right). They do not represent the best fit to the observations, but stress the bimodality of the system (see e.g. NICHOLLS, 1979, Figure 4).

**Graphical predictions:** The discrete dynamics of this system can be traced by a graphical staircase construction in the plane spanned by the  $I_{t+1}$ -ordinate and  $I_t$ -abscissa. In this plane the function (2.1)  $I_{t+1} = f(I_t)$  is plotted together with the diagonal  $I_{t+1} = I_t$ . A graphical iteration (Fig. 1, right) demands the following steps, which start from an initial value  $I_{t=0}$  on the  $I_t$ -axis: (i) One moves vertically to the graph  $I_{t+1} = f(I_t)$ ; (ii) One goes horizontally from this point to the diagonal  $I_{t+1} = I_t$  (i.e.  $I_{t+1}$  is trasformed back to the  $I_t$ -axis) and proceeds by repeating the steps (i) and (ii).



● **Figure 1** Intensities of the El Niño/Southern Oscillation phenomenon (data from QUINN et al. 1978), left: number distribution of ordered pairs  $(I(t), I(t+1))$  of 120 intensity values of successive years; right: one-dimensional function approximating the ordered intensity pairs as an analytical climate iteration. A graphical iteration illustrates a sequence of six years starting from a "no" event situation.

Fixed points occur where the graph of the polynomial function (2.1) intersects the diagonal  $I_{t+1} = I_t = \bar{I}$ ; i.e.

$$M_0 + M_1 \bar{I} + M_2 \bar{I}^2 = 0 \quad (2.2)$$

There are two of them at the intensities  $\bar{I}_1 = 1$  and  $\bar{I}_2 = 4$ , which belong to the “no” and “moderate to strong” category. These positions appear physically reasonable; their stability properties will be discussed in more detail in Section 3.

**A solution:** An analytical solution of the iteration (2.1) is known for the particular set of coefficients (ULAM and von NEUMANN, 1947):

$$I_t = 2 (1 + \cos 2^{t+1} \phi) \quad (2.3)$$

where  $\phi$  depends on the initial value  $I_t$  at  $t=0$ . Any two trajectories starting close to each other separate at an exponential rate showing the strong sensitivity of the system on initial conditions; i.e. the fixed points of “no” and “strong” El Nino years,  $\bar{I}_1$  and  $\bar{I}_2$ , are unstable. In particular a rational  $\phi$  leads to an infinite number of periodic orbits. Furthermore, most points of the iterations (2.3) visit every region of the intensity interval,  $0 \leq I \leq 4$ , with almost equal probability; but the boundaries are most often frequented. This is known as chaotic behaviour within the intensity interval, which occurs in purest form whenever an extremum of a quadratic function is mapped onto an unstable fixed point (GUMOWSKI and MIRA, 1980); i.e. starting from the extremum  $I_c = 2$  one enters the fix point  $\bar{I}_2 = 4$  after two iterations (see Figure 1, right).

However, pure chaos is not the dominant feature of the interannual variability of the tropical climate system as suggested by this selection of parameters. Observed spectra, in particular of the sea surface temperature, exhibit a major peak at the period of about 3 to 3.5 years (RASMUSSEN and CARPENTER, 1982) with other periods also existing. But periodicity and noisy periodicity are common features of this type of discrete dynamical model. They appear, if the parameters are changed.

**A physical iteration:** If the empirical coefficients  $M_0$  to  $M_2$  vary by the same factor, the fixed points (2.2) remain unchanged. The dynamics, however, is modified considerably, because the extremum does no longer iterate to unstable fixed points. Such a further evaluation of the discrete model dynamics is reasonable, if the intensity can be interpreted as a thermal energy anomaly  $c T_t$ , where the thermal inertia,  $c$ , corresponds to an ocean surface layer of depth  $h$  (in meters)

$$c \sim 0.04 h \quad (2.4)$$

in  $\text{Joule K}^{-1} \text{m}^{-2}$  or  $10^8 \text{ kg K}^{-1} \text{s}^{-2}$ . Now, assume a representative layer depth (e.g.  $h \sim 100 \text{ m}$ ) for a calibration of (2.1), which should correspond to the water mass affected by El Nino; and let the related temperature anomalies  $T$  (in degrees Kelvin) cover the interval  $0 \leq T \leq 10 \text{ K}$  (instead of  $0 \leq I \leq 4$ ), which is suggested by the observed temperature rise from  $21^\circ \text{C}$  (July 81) to about  $30^\circ \text{C}$  (April 83) in 15 m depth at  $0^\circ, 110^\circ \text{W}$  (HALPERN et al., 1983). Then one obtains the climate iteration

$$c T_{t+1} - c T_t = m_0 + m_1 T_t + m_2 T_t^2 + \dots \quad (2.5a)$$

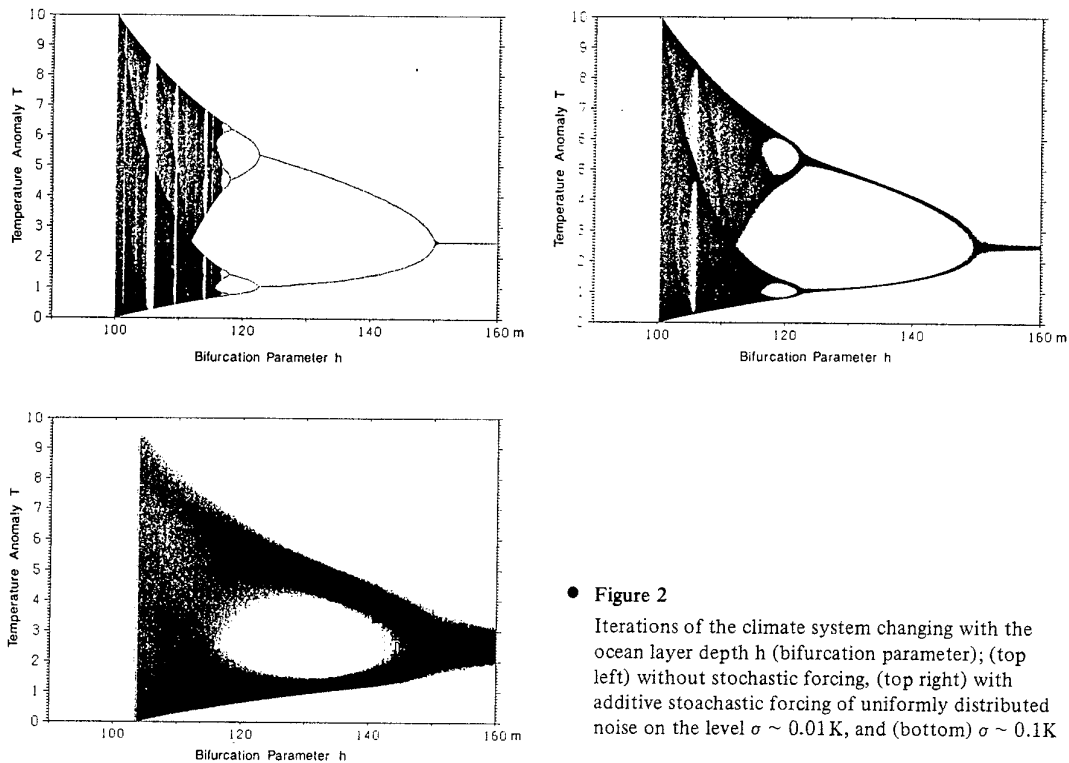
where  $m_0 = 40 \text{ Joule m}^{-2}$ ,  $m_1 = -20 \text{ Joule K}^{-1} \text{m}^{-2}$ ,  $m_2 = 1.6 \text{ Joule K}^{-2} \text{m}^{-2}$  and  $c = 4 \text{ Joule K}^{-1} \text{m}^{-2}$ . The thermal inertia,  $c$ , or ocean layer depth,  $h$ , enters as a physical property into all empirically deduced parameters,  $M_j$ , of the iteration (2.1); but in the following,  $c$  or  $h$  serve as the basic feedback parameters of the system only as defined by (2.5). This does not confine the results, because small changes of any parameter lead to similar modifications of the time evolution of the system and its statistic.

Furthermore we consider only terms up to the quadratic power, although the contribution of higher order terms allows a better fit to the observations (Figure 1, left). Since locally every nonlinear system is quadratic, the higher orders may be neglected. They, however, can be reintroduced as random forces (discussed in Section 4). The resulting quadratic iteration of first order (i.e. from  $t$  to  $t+1$ ) describes a time evolution of a discrete climate system, which is not to be mistaken with a discretization of a continuous time evolution equation:

$$T_{t+1} = T_t + c^{-1} (m_0 + m_1 \cdot T_t + m_2 \cdot T_t^2) + E_t = f(T_t) + E_t \quad (2.5b)$$

where the bifurcation parameter  $c$  corresponds to the related layer depth  $0.04 h$  ( $h$  in meters). The stochastic fluctuations,  $E_t$ , are added to explicitly represent random noise and errors. They may be due to the parameterizations involved in deducing the climate iteration, higher order terms, or external forcing. Discussions on their influence are postponed to Section 4.

Most of the characteristic features of the climate iteration (2.5) can be shown in one figure (Figure 2, COLLET and ECKMANN, 1981). For the selected  $m_j$ -parameters 1000 iterations are plotted after the initial 200 transients at each bifurcation parameter  $h$  (ocean layer depth) increasing from  $h = 100$  m depths by  $0.05$  m steps. The 1000 iterations can be interpreted as a frequency distribution at each layer depth; darker areas represent higher probability (densities) of the system to be found in the related temperature state. One observes that the climate system iterates within (periodic) temperature intervals or on periodic points, both of which bifurcate at certain  $h$ -values (indicated on the abscissa, Figure 2). From  $h_{(0)} = 100$  m to  $h = h_\infty$ , the single noisy or chaotic temperature interval bifurcates into a cascade of intervals with a period doubling sequence (see Section 4). At a critical value,  $h_\infty$ , an



● **Figure 2**  
Iterations of the climate system changing with the ocean layer depth  $h$  (bifurcation parameter); (top left) without stochastic forcing, (top right) with additive stochastic forcing of uniformly distributed noise on the level  $\sigma \sim 0.01$  K, and (bottom)  $\sigma \sim 0.1$  K

inverse cascade of pairwise merging periodic points evolves (from an infinite period to period one), until a single steady state solution,  $\bar{T}_1 = 2.5$  K, which occurs at  $h_1 = 150$  m, is reached.

Although the iterations exhibit a detailed structure, only features relevant to climate modelling will be discussed in the following sections: the limited range of allowed temperature values (Section 3), the probability of finding the system in certain temperature states and the effect of stochastic forcing (Section 4).

### 3 Predictions of first kind: interval of attraction and invariant intervals

The predictions of first kind describe the iterations of the climate variable  $T_t$  at fixed external parameters or boundary conditions and depend on the choice of the initial value  $T_{t=0}$ . These iterations can be visualized as described in Section 2 (Figure 1, right).

Fixed points (equilibria, stationary states) of the iterations are given by the conditions  $T_t = T_{t+1} = \bar{T}$ . These points are identical with the intersections of the function  $T_{t+1} = f(T_t)$  with the diagonal  $T_{t+1} = T_t$ . There are two of them and their locus in the  $(T, m)$ -space is

$$\bar{T}_{1,2} = -\frac{1}{2m_2} (m_1 \pm (m_1^2 - 4m_0 m_2)^{1/2}) \quad (3.1)$$

Their value is independent of the thermal inertia  $c$  or ocean layer depth  $h$  (bifurcation parameter). For the model constants  $m_j$  derived from the observed intensity iteration, one obtains  $\bar{T}_1 = 10$  K and  $\bar{T}_2 = 2.5$  K characterizing the strong El Nino and "no-event" situation, respectively. Stability of these fixed points to small perturbations  $T_t = \bar{T} + \Delta_t$  is discovered by Taylor series expansion, which describes the slope of  $T_{t+1} = f(T_t)$  at the intersection with the diagonal  $T_{t+1} = T_t$ . For small  $\Delta_t$  one obtains  $T_{t+1} = \bar{T} + \Delta_{t+1} = f(\bar{T} + \Delta_t) = f(\bar{T}) + f'(\bar{T}) \Delta_t + \dots = \bar{T} + f'(\bar{T}) \Delta_t + \dots$ . This gives the stability conditions

$$\begin{aligned} \frac{\Delta_{t+1}}{\Delta_t} &= f'(\bar{T}) = 1 + c^{-1} (m_1 + 2m_2 \bar{T}) \\ &= 1 - c^{-1} (\pm(m_1^2 - 4m_0 m_2)^{1/2}) \end{aligned} \quad (3.2)$$

with  $f'(\bar{T}) = df/dt|_{\bar{T}}$ . If  $|f'(\bar{T})| > 1$ , successive iterations starting near  $\bar{T}$  move further away from it; i.e.  $\bar{T}$  is unstable. If  $|f'(\bar{T})| < 1$ , the iterations converge and  $\bar{T}$  is stable. Applied to the climate iteration this means that the fixed point  $\bar{T}_2 = 10$  K (related to the negative sign of the square root) is unstable, because  $c > 0$ . The fixed point "no event" (i.e.  $\bar{T}_1 = 2.5$  K) is stable for  $2 < 12/c < 0$ ; this equivalent for an ocean layer depth up to 150 m; i.e. for  $150 \text{ m} \leq h < \infty$ , whence  $|f'(\bar{T})| < 1$ . Further discussions on the stability of the fixed point  $\bar{T}_1 = 2.5$  K follow in Section 4.

**Interval of attraction:** An interval or basin of attraction is defined by the set of those initial values  $T_{t=0}$ , where related  $T$ -trajectories remain in or are mapped into smaller parts of it. The boundaries of the attracting interval may change with varying inertia  $c$  or layer depth  $h$ . Accordingly the internal structure of the time evolution may also change.

One limit of the  $T$ -interval of attraction is the unstable fixed point  $\bar{T}_2$  ( $\sim 10$  K), which is independent of the thermal inertia  $c$ . This limit is an upper boundary, because initial values  $T_{t=0} < \bar{T}_2$  are repelled from  $\bar{T}_2$  and attracted by the fixed point  $\bar{T}_1 < \bar{T}_2$ ; but initial values  $T_{t=0} > \bar{T}_2$  move towards infinity. The lower limit of the attracting interval is determined by the first backward iteration of the unstable fixed point  $\bar{T}_2$ ; i.e.  $\bar{T}_0 = f^{(-1)}(\bar{T}_2)$  or  $\bar{T}_2 = f(\bar{T}_0)$ :

$$\bar{T}_2 = \bar{T}_0 + c^{-1} (m_0 + m_1 \bar{T}_0 + m_2 \bar{T}_0^2) \quad (3.3)$$

As the climate iteration (2.5) is not invertible, there are two solutions. The first yields

$$\bar{T}_0 = \bar{T}_1 - c/m_2 \quad (3.4)$$

It depends linearly on the thermal inertia  $c$  or ocean layer depth  $h$ . The second one ( $\bar{T}_2$ ) is trivial, because it characterizes repeated iterations of exactly the unstable fixed point. Thus, also  $\bar{T}_0$  is mapped onto the unstable fixed point  $\bar{T}_2$ , where future iterations remain.

Smaller (larger) initial values than  $\bar{T}_0$  move above (below) the upper limit  $\bar{T}_2$ , from where future iterations are repelled towards infinity (tend towards further inside). Summarizing: Successive iterations starting from the maximum interval of attraction cannot escape:

$$\bar{T}_0 \leq T_t \leq \bar{T}_2 \quad (3.5)$$

Initial values below the lower temperature boundary ( $T_{t=0} < \bar{T}_0$ ) lead to unbounded iterations, because  $T_{t+1}/T_t > 1$  (2.5). Above the upper temperature boundary ( $T_{t=0} > \bar{T}_2$ ) the first iteration yields  $T_{t=1} < \bar{T}_0$  and the same argument holds. It should be noted that the lower temperature boundary ( $\bar{T}_0 = 2.5 - 0.025 h$ ) decreases with increasing thermal inertia or layer depth  $h$ , whereas the upper limit remains fixed at  $\bar{T}_2$ ; i.e. a large inertia or layer depth  $h$  makes the climate iteration at the selected parameter values more resilient with respect to large negative temperature departures, but not to positive ones.

**Invariant intervals:** The maximum interval of attraction contains a smaller interval and subintervals, to which the time iterations tend. Furthermore, trajectories remain in these intervals once they are captured; these intervals are invariant, because they are mapped onto itself. The  $T$ -boundaries of the invariant intervals can be determined from iteration of the critical or limiting point, which is the extremum of the  $f(T_t)$ -parabola, determined by  $df/dT = 0$ :

$$T_c = -\frac{1}{2m_2} (c + m_1) \quad (3.6)$$

For the selected parameter values the critical temperature  $T_c$  is a minimum, because  $df^2/dt^2 > 0$ ; its magnitude varies linearly with the bifurcation parameter  $c$ , or the ocean layer depth ( $T_c = 6.25 - 0.0125 h$ ).

As iterations cannot drop below the critical point, its first and second iterate  $f(T_c)$  and  $f^{(2)}(T_c)$  cannot be surpassed in either direction; i.e. iterations must lie between  $f^{(1)}(T_c)$  and  $f^{(2)}(T_c)$ . These iterates of the critical point define temperature limits, from which all  $T_t$ -values larger than  $T_c$  cannot escape. The first iterate defines the lower bound of  $T_t$ , which is given by

$$f(T_c) = \frac{m_0}{c} - \frac{\left(\frac{m_1}{c} + 1\right)^2}{4m_2/c} \quad (3.7)$$

The second iterate defines the upper bound,

$$f^{(2)}(T_c) = f(f(T_c)) \quad (3.8)$$

This leads to the invariant interval mapped onto itself:

$$f(T_c) \geq T_t \geq f^{(2)}(T_c) \quad (3.9)$$

Both T-intervals of attraction (3.5) and invariance (3.9) do not exist for all bifurcation parameter values  $c$ ; the time evolution of the climate iteration is constrained within certain parameter domains. Their lower limits concur at  $c_{(0)}, h_{(0)}$  where both intervals coincide; i.e.  $\bar{T}_0 = f^{(1)}(T_c)$  and  $\bar{T}_2 = f^{(2)}(T_c)$ . This yields

$$c_{(0)} = \frac{1}{3} (m_1^2 - 4m_0 m_2)^{1/2} \quad (3.10)$$

For the selected parameters  $m_j$  and for  $c = 0.04 h$  (2.4) one obtains the limit at  $h_{(0)} = 100$  m. If the bifurcation parameter  $c$  or  $h$  decreases below this value, the temperature iterations, although captured in the invariant interval, leave the basin of attraction; i.e. they are repelled and become unbounded. This happens if the inertia of the system is sufficiently small. Vice versa, for larger ( $h > 100$  m) inertia or ocean layer depth the basin of attraction contains the invariant interval, towards which trajectories tend, stable orbits and the equilibrium  $\bar{T}_1$ . A natural lower bound for the interval of attraction is the infinitely large inertia or ocean depth  $c$  or  $h \rightarrow \infty$ , where the lower (upper) T-limit of the attracting interval rises to  $\bar{T}_0 = -\infty$  (remains at  $\bar{T}_2$ ).

**Climate modelling aspects:** The existence of a basin of attraction and of embedded invariant intervals can be reflected in what we may actually observe. The invariant interval (3.9) defines the limits of the frequency distribution of the climate iteration; i.e. El Nino/Southern Oscillation events or intensities should – under regular circumstances without external forcing – remain within these bounds (e.g. Figure 1). But any external event can push the system outside these limits (e.g. by volcanic activity); the width of the attracting interval, however, guarantees a certain resilience of the climate system and defines the range of such external shocks being absorbed. Thus, in climate analysis one may distinguish between the limits of a basin or interval, where the regular and undisturbed evolution takes place, (which may hardly be observed), and the bounds of an attracting basin where shocks are absorbed to return the system to the basin of its regular evolution.

#### 4 Time evolution: periodicity, noisy periodicity and stochastic fluctuations

The climate iteration reveals two different modes of time evolutions: Iterations which start within the attracting interval become periodic, if the bifurcation parameter lies in the domain  $h_\infty < h < \infty$ . If  $h_{(0)} = 100$  m  $< h < h_\infty$ , iterations become chaotic with bands of noisy periodicity occurring. For  $0 < h < 100$  m iterations tend to infinity.

**Periodicity ( $h_\infty < h < \infty$ ):** A decreasing thermal inertia or layer depth  $h$  reveals a cascade of period doubling bifurcations. The fixed point  $\bar{T}_1$  remains stable for  $h_1 < h < \infty$ , but becomes unstable at  $h_1 = 150$  m (Section 3), where bifurcation into a period 2-cycle,  $T_{t+2} = f(f(T_t))$ , occurs. The related two temperature values ( $T_a, T_b$ ) are two stable solutions of  $T_t = T_{t+2} = f^{(2)}(T_t)$ . These equilibria are intersections of the diagonal ( $T_{t+2} = T_t$ ) with the graph  $T_{t+2} = f^{(2)}(T_t)$ . They and their stability (slope of tangent) may be visualized in the  $(T_{t+2}, T_t)$ -plane and evaluated in analogy to the period one fixed points  $T_1, T_2$  (Section 3).

The 2-cycle loses stability and bifurcates into a stable orbit of a period  $p = 2^2$  cycle at  $h_2$ , which again becomes unstable to bifurcate at  $h_3$  into a  $p = 2^3$  cycle, etc. The bifurcation parameters of stable  $2^n$ -cycles converge from  $h_1$  to the limit  $h_n = h_\infty$  with  $n \rightarrow \infty$  at a well defined rate. This was first found numerically by GROSSMANN and THOMAE (1977); FEIGENBAUM (1978, 1979) showed that the convergence rate of the bifurcation parameter is identical for an entire class of iterations which are characterized by a single maximum or minimum.

**Noisy periodicity ( $h_{(0)} < h < h_\infty$ ):** At the upper parameter limit,  $h_{(1)} = 100$  m, the invariant interval coincides with the basin of attraction and noisy orbits (of period 1) are observed. In Section 2 the



related analytical solution (2.3) and its properties have been discussed; e.g. the extremum  $T_c$  being mapped onto the unstable fixed point,  $\bar{T}_2$ , after the second iteration:

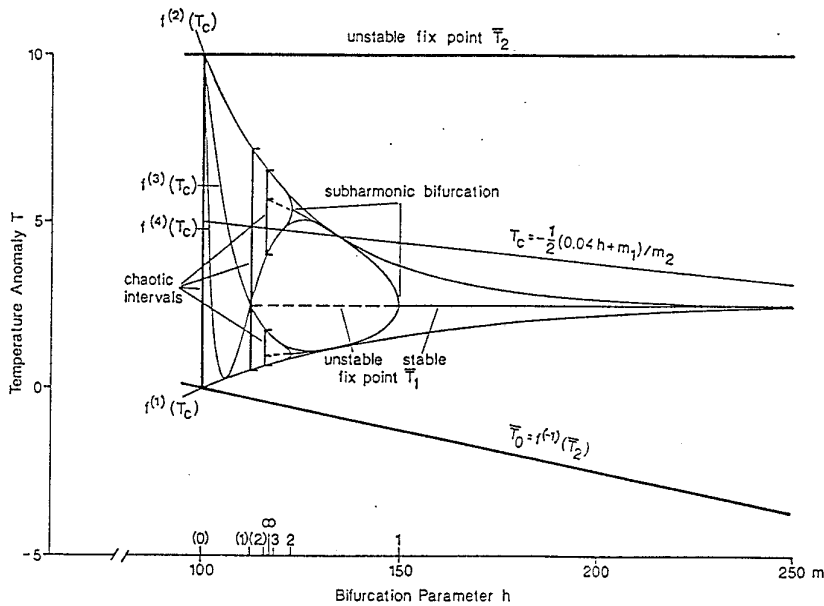
$$f^{(2)}(T_c) = \bar{T}_2 \quad (4.1a)$$

Increasing the parameter (or layer depth) from  $h_{(0)}$  to  $h_\infty$  leads to a series of reverse bifurcations of noisy temperature intervals (or bands), which also exhibit period doubling. At  $h_{(1)}$  the single noisy band (2.3) splits into two noisy intervals, which have one boundary in common,  $(\bar{T}_1)$ :  $f^{(1)}(T_c) \leq T \leq \bar{T}_1$  and  $\bar{T}_1 \leq T \leq f^{(2)}(T_c)$ . They are alternately visited by the trajectory. The value of this bifurcation parameter satisfies the condition that the extremum is mapped onto an unstable fixed point after the third iteration

$$f^{(3)}(T_c) = \bar{T}_2 \quad (4.1b)$$

Again, if  $h$  is larger (smaller) than  $h_{(1)}$ , the extrema  $T_c$  do no longer iterate onto the unstable fixed points ( $\bar{T}_2$  or  $\bar{T}_0$ ), but into separated (overlapping) temperature intervals (Figures 2 and 3). This leads to irregular jumps between the two  $T$ -intervals, which destroy the pure period 2 chaos (THOMAE and GROSSMANN, 1981).

Increasing the bifurcation parameter  $c$  or  $h$  further, the two noisy temperature intervals are split into four at  $h_{(2)}$  satisfying  $f^{(4)}(T_c) = T_2$ , the four bands split into eight etc., until they converge at  $c_\infty$  or  $h_\infty$ . This is the same limiting value as deduced for the period doubling bifurcations of the stable orbits and the convergence rate follows the same law. The noisy periods  $k$  at  $h_{(k)}$  are the counterparts of the stable period  $k$  orbits, where stable fixed points of the iteration  $f^{(k)}(T_i)$  are separated by the unstable



● **Figure 3** Schematic diagram of the structure of the climate iteration in the parameter-state space: basin of attraction  $\bar{T}_2 \geq T \geq \bar{T}_0$  (thick lines), invariant interval  $f^{(2)}(T_c) \geq T \geq f^{(1)}(T_c)$  (thin lines). The numbers on the abscissa indicate the bifurcations from the stable fixed point,  $\bar{T}_1 = 2.5\text{K}$ , to orbits of period one, two, three, etc., and the bifurcations of irregular orbits in temperature intervals (from right to left). Note the coincidence of the "darker trails" in Figure 2, which indicate high probability densities, with the iterates  $f^{(k)}(T_c)$  of the extremum  $T_c$ .

ones of the iteration  $f^{(k-1)}(T_t)$ . These unstable fixed points also separate the chaotic temperature intervals. Furthermore, stable orbits exist for a parameter range  $(h_k, h_{k-1})$ , whereas pure chaos is found at parameter values  $h_{(k)}$ .

**Stochastic fluctuations:** The parameterization of the climate system and its time evolution (section 2), which leads to the discrete iteration (2.1, 2.5) may include errors or stochastic forcing due to those processes, which remain unresolved in time. Their influence in terms of random noise  $E_t$

$$T_{t+1} = f(T_t) + E_t \quad (4.2)$$

can quite generally be assumed as an additive forcing (CRUTCHFIELD et al., 1982). Taking  $E_t$  as a uniformly distributed random temperature with zero mean and standard deviation (or noise level),  $\sigma$ , one obtains the following results (Figure 2). As expected, the random fluctuations reduce the detailed features of the iteration (2.5). The trajectories in the periodic regime ( $h_\infty \leq h < \infty$ ) broaden into intervals and become similar to the chaotic bands of noisy periodicity (Figure 2). The chaotic regime,  $h_{(1)} < h \leq h_\infty$ , however, does not become periodic; almost all periodic windows disappear with the exception of period 3, which is still visible even at  $\sigma \sim 0.01$  K. With increasing noise level the number of resolvable periodic orbits and chaotic intervals is diminished. An almost continuous transition across  $c_\infty$  or  $h_\infty$  develops from the randomly disturbed regimes or periodicity to the reverse bifurcations of noisy periodicity. At  $\sigma \sim 0.1$  K, only two bands remain in the invariant interval, because the random fluctuations destroy bifurcations and reverse bifurcations of the periodic and chaotic regimes except for their transition to the period 2 cycle. Both regimes merge at higher noise levels. The distinction between periodic orbits and chaotic intervals is not straight forward, if random forcing is added to the discrete climate system. At prescribed boundary conditions ( $c$  or  $h$ ) the additive fluctuations change the deterministic evolution of the climate, as if it jumps to the attractors of the adjacent parameters. But this effects only the local stability properties of the time evolution. However, one observes (Figure 2) that the global structure of the attractor basin with the attracting and invariant intervals (Section 3) remains stable under the influence of random fluctuations with small to moderate levels.

**Climate modelling aspects:** (i) The probability to find the system in preferred climate states is another essential of iterative climate models, besides the significance of the attracting and invariant intervals (Section 3). The location of probability density maxima can simply be evaluated, because the extremum of  $f(T_t)$  occurring at  $T_c$  is parabolic and smooth. Due to this fact the first few iterates of a relatively wide range of initial values neighbouring  $T_c$  do not vary strongly; i.e. the system iterates preferably onto temperature states near  $f^{(1)}(T_c)$ ,  $f^{(2)}(T_c)$ , etc.. Thus, for example, the (one-sided) neighbourhoods of the two boundaries of the basic invariant interval are most often frequented. This corresponds to the observed u-shaped frequency distribution of El Niño/Southern Oscillation events (Section 2; cumulating the observations in Figure 1).

(ii) Furthermore, windows with periodic iterations open within the chaotic regime  $h_{(0)} = 100 \text{ m} \leq h < h_\infty$  (Figure 2). The most dominant feature of this kind is the period 3 window, which is recognizable even if stochastic forcing is added (Figure 2). These stable iterations of periodicity,  $n$ , appear in the irregular domain, whenever the  $n$ -th iterate of the extremum returns to itself. Thus, it is the condition  $f^{(k+n)}(T_c) = f^{(k)}(T_c)$ , which opens the windows in the parameter-state space. Their number increases with  $n$ , but its parameter width decreases (see CRUTCHFIELD, FARMER and HUBERMAN, 1982 and COLLET and ECKMANN, 1980 for further details). The particularly wide window of period 3 is of more general significance in the context of nonlinear maps ("period three implies chaos", LI and YORKE, 1975) and might also be responsible for the observed recurrence time of 3.2 years of the inset of strong, moderate, weak and very weak El Ninos (QUINN et al., 1978). Correspondingly, OORT (1983) observes a strong variability of the vertical mean temperatures of northern and southern hemisphere near a period of 40 months.

(iii) Intermittency is another feature characterizing the time evolution of the observed El Nino/Southern Oscillation and the related quadratic iteration. El Nino episodes with almost regular recurrence times between two and four years are documented for the recent 20 to 30 years, and before the turn of the century; irregularly long time intervals elapse between El Ninos from the twenties to the forties. The parameter range opening the period 3 window for the El Nino iterations reveals a qualitatively similar time evolution with a sequence of more quiescent events replacing strong El Nino/anti El Nino episodes. Such time evolution can be associated with the well known  $1/f$ -noise phenomenon and inverse tangent bifurcations.

## 5 Conclusion

Smoothly varying climate systems are the common way to model the climate evolution; iterative climate systems, however, simulate only (i) the intersections of a smooth trajectory with a suitable cross-section of the climate phase space or (ii) a sequence of local extrema of the continuous trajectory. This reduces the possibility of an immediate physical interpretation, because only subsets of the whole system and its time evolution are described. In this sense iterative climate models do not originate from discretizing a continuous system but are a parameterization of the smooth process, which is confined to dominant model structures.

An iterative (quadratic) climate system is deduced from observed intensities of the El Nino/Southern Oscillation phenomenon and analysed as a prototype. The analysis stresses structures relevant to climate modelling. They are related to the predicitions of first and second kind: the locus of the basin of attraction in the parameter-state space and the embedded invariant intervals, which irregular iterations do not leave once captured. A sufficiently large inertia (as one of the possible bifurcation parameters) forces the climate iteration towards a single stable fixed point by attracting initial values from a large basin – no El Nino would occur. A reduced inertia (or shallow ocean), however, generates irregular iterations with excursions to temperatures, which represent El Nino events. They become increasingly periodic and noisy. This coincides with a reduction of the attraction basin and a simultaneous broadening of the temperature interval where iterations remain after the memory of their initial value is lost. Details of the local behaviour are a complex mathematical problem. But, as these local structures are modified by small random noise, they may be considered less significant for climate modelling. However, the basin of attraction and the invariant interval are not effected by stochastic forcing. Therefore, they seem to be structures relevant for climate systems analysis.

## Acknowledgement

Thanks are due to Mr. H. HAUG for computing and plotting assistance and Mrs. M. SCHOLZ and Ms. F. NIKOU for typing.

## List of symbols

$I$	annual intensity of El Nino/Southern Oscillation events
$T$	temperature anomaly (in Kelvin) related to intensity $I$
$c$ or $h$	bifurcation parameter: thermal inertia or ocean surface layer depth
$M_0, M_1, M_2$	expansion coefficients of intensity iteration
$m_0, m_1, m_2$	expansion coefficients of temperature iteration
$\bar{T}_1, \bar{T}_2, \bar{T}_0, T_c$	stable, unstable fixed point, backward iterate of $\bar{T}_2$ , extremum or critical point of $f(T_t)$

$f(T_t), f^{(k)}(T_t), f'(T_t)$	climate iteration, k-th iteration, first derivative
$h_k, h_{(k)}, h_\infty$	bifurcations of periodic iterations, bifurcations of periodic intervals with irregular orbits, limiting or critical value.
$E_t, \sigma$	additive stochastic fluctuations, level of uniformly distributed noise.

#### Indices:

t, t+1, t+2	time iterations
-------------	-----------------

#### References

- BENZI, R., J. P. PANDOLFO and A. SUTERA, 1981: Further application of the theory of stochastic perturbation of deterministic systems to simple climate models. *Quart. J. R. Met. Soc.* **107**, 549–559.
- COLLET, P. and J. P. ECKMANN, 1980: Iterated maps on the interval as dynamical systems. Birkhäuser, 248 pp.
- CRUTCHFIELD, J. P., J. D. FARMER and B. A. HUBERMAN, 1982: Fluctuations and simple chaotic dynamics. *Physics Reports* **92**, 45–82.
- ECKMANN, J.-P., 1981: Roads to turbulence in dissipative dynamical systems. *Rev. Modern Phys.* **53**, 643–654.
- FEIGENBAUM, M. J., 1978: Quantitative universality for a class of nonlinear transformations. *J. Stat. Phys.* **19**, 25–52.
- FRAEDRICH, K., 1978: Structural and stochastic analysis of a zero-dimensional climate system. *Quart. J. R. Met. Soc.* **104**, 461–474.
- FRAEDRICH, K., 1979: Catastrophes and resilience of a zero-dimensional climate system with ice-albedo and greenhouse feedback. *Quart. J. R. Met. Soc.* **105**, 147–167.
- GROSSMANN, S. and S. THOMAE, 1977: Invariant distributions and stationary correlation functions. *Z. Naturforsch.* **32a**, 1353–1363.
- GUMOWSKI, I. and C. MIRA, 1980: Recurrences and discrete dynamic systems. *Lecture Notes in Mathematics* **809**, Springer Verlag.
- HALPERS, D., S. AP. HAYES, A. LEETMAA, D. V. HANSEN and S.G.H. PHILANDER, 1983: Oceanographic observations of the 1982 warming of the tropical eastern Pacific. *Science* **221**, 1173–1175.
- HELLEMAN, R.H.G., 1980: Self-generated chaotic behaviour in non-linear mechanics. *Fundamental Problems in Statistical Mechanics* **5** (E.G.D. COHEN, Ed.), North-Holland Publ. Comp., 165–233.
- LI, T. Y. and J. YORKE, 1985: Period three implies chaos. *Amer. Math. Monthly* **82**, 985–992.
- LORENZ, E. N., 1963: Deterministic non periodic flow. *J. Atmos. Sci.* **20**, 130–141.
- LORENZ, E. N., 1964: The problem of deducing the climate from the governing equations. *Tellus* **16**, 1–11.
- MAY, R. M., 1976: Simple mathematical models with very complicated dynamics. *Nature* **261**, 459–467.
- NICHOLLS, N., 1979: A simple air-sea interaction model. *Quart. J. R. Met. Soc.* **105**, 93–105.
- OORT, A. 1983: Global atmospheric circulation statistics 1958–1973. NOAA Professional Paper **14**, US Department of Commerce, 180 pp.
- OTT, E., 1981: Strange attractors and chaotic motions of dynamical systems. *Rev. Modern Phys.* **53**, 655–671.
- QUINN, W. H., D. O. ZOPF, K. S. SHORT and R.T.W. KUO YANG, 1978: Historical trends and statistics of the southern oscillation, El Nino, and Indonesian droughts. *Fishery Bulletin* **76**, 663–678.
- RASMUSSEN, E. M., 1984: El Nino: The ocean/atmosphere connection. *Oceanus* **27**, 5–12.
- RASMUSSEN, E. M. and T. H. CARPENTER, 1982: Variations in tropical sea surface temperature and surface wind fields associated with the Southern Oscillation/El Nino. *Mon. Wea. Rev.* **110**, 354–384.
- SUTERA, A., 1981: On stochastic perturbation and long-term climate behaviour. *Quart. J. R. Met. Soc.* **107**, 137–151.
- THOMAE, S. and S. GROSSMANN, 1981: Correlations and spectra of periodic chaos generated by the logistic parabola. *J. Statist. Phys.* **26**, 485–504.
- ULAM, S. A. and J. von NEUMANN, 1947: On combinations of stochastic and deterministic processes. *Bull. Amer. Math. Soc.* **53**, 1120.
- VALLIS, G. K., 1986: El Nino: a chaotic dynamical system? *Science* **232**, 243–245.